

# Influence of Majorana-parity degeneracy on the boundary Berezinskii-Kosterlitz-Thouless quantum phase transition of a dissipative resonant level

Gu Zhang,<sup>1,\*</sup> Zhan Cao,<sup>1</sup> and Dong E. Liu<sup>2,1,3,4,†</sup>

<sup>1</sup>Beijing Academy of Quantum Information Sciences, Beijing 100193, China

<sup>2</sup>State Key Laboratory of Low Dimensional Quantum Physics,

Department of Physics, Tsinghua University, Beijing, 100084, China

<sup>3</sup>Frontier Science Center for Quantum Information, Beijing 100184, China

<sup>4</sup>Hefei National Laboratory, Hefei 230088, China

(Dated: March 21, 2023)

The interplay between a topological degeneracy and the residue degeneracy (also known as the residue entropy) of quantum criticality remains as an important but not thoroughly understood topic. We find that the degeneracy of topological parity, provided by a Majorana zero mode pair, relaxes the otherwise strictly requested symmetry requirement, to observe the boundary Berezinskii-Kosterlitz-Thouless (BKT) quantum phase transition (QPT) of a dissipative resonant level. Our work indicates that the topological-parity degeneracy can be potentially viewed as an auxiliary symmetry that realizes a robust boundary QPT. The relaxation of the symmetry requirement extends the transition from a point to a finite area, thus greatly reducing the difficulty to experimentally observe the QPT. This topology-involved exotic BKT phase diagram, on the other hand, provides a piece of convincing evidence for a Majorana zero mode.

**Introduction**—Boundary quantum phase transitions (QPTs) [1, 2] are special QPTs triggered by the change of boundary conditions. Similar as the bulk ones, boundary QPTs normally involve symmetries. For instance, in multi-channel Kondo [3–8], Luttinger liquid resonant [9], and dissipative resonant level [10–12] models, the observation of quantum critical point (QCP), i.e. the point that separates two zero-temperature phases [13], requires the impurity (a quantum dot or magnetic impurity) to symmetrically couple to involved leads. Actually, the symmetric coupling that triggers quantum frustration at QCP produces a non-trivial residue degeneracy, which is another important feature of QPT [1, 4]. This residue degeneracy, heavily focused on recently as a QPT-induced “anyon” [14–18], has been proposed as an amplifier of topological non-triviality [19]. As another example, a Berezinskii-Kosterlitz-Thouless (BKT) transition is predicted in a dissipative resonant level model (DRLM) [12, 20], between the ballistic-transmission and isolated-impurity phases. Its observation, importantly, also requires perfectly symmetric lead-dot couplings, since its ballistic-transmission phase consists of solely a line of QCPs. This fine-tuning prerequisite of symmetry is among the difficulties to observe this BKT QPT. To the best of our knowledge, a BKT-type boundary QPT, has not yet been reported experimentally.

On the other hand, a pair of Majorana zero modes (MZMs), predicted to exist at end points of a nanowire heterostructure [21–23] and vortices of a topological superconductor [24, 25], is known to provide a non-locally defined topological degeneracy, given a long enough inter-MZM distance. This topological degeneracy, distinct from a trivially local one, is among the key elements of topological quantum computation [26]. Exploring the intricate influences of topological degeneracy on the residue degeneracy in QPTs, where symmetry is a prerequisite, constitutes a compelling avenue of investigation. A crucial line of inquiry involves investigating the

potential role of topological degeneracy as an auxiliary symmetry capable of reinstating boundary QPTs that have been undermined by asymmetry.

**Summary of main results:** In this work, we visit this topic by investigating the influence of topological-parity degeneracy on the boundary BKT QPT in a DRLM. Without the topological-parity degeneracy, it is known that the BKT transition of a DRLM requires a perfect symmetry between two involved leads. Surprisingly, as among our central results, this strict symmetry requirement (to observe the BKT QPT) is remarkably relaxed, by coupling an MZM to the dot of the DRLM [see Fig. 2 that is distinct from Fig. 1(b)]. With Coulomb gas renormalization group (RG) equations and g-theorem [27, 28], we further prove that the relaxation of symmetry requirement is a direct consequence of the topological-parity degeneracy, with which the left-right asymmetry becomes irrelevant near the strong-tunneling fixed point. Our work, as far as we know, is pioneering in studying the interplay between topological-parity degeneracy and boundary QPTs where symmetries are otherwise strictly requested. In addition, the broadened ballistic-transmission phase space (Fig. 2) greatly reduces the experimental difficulty to observe the BKT QPT of a DRLM. Remarkably, the phase diagram featuring MZMs, which greatly contrasts that of a regular DRLM, provides a clear and unequivocal indicator for detecting the presence of MZMs.

**Model**—The system we consider [with the Hamiltonian  $H = H_{\text{leads}} + H_{\text{impurity}} + H_{\text{T}}$ , see Fig. 1(a)] contains two dissipative leads ( $H_{\text{leads}}$ ) that couple to ( $H_{\text{T}}$ ) a Majorana-contained impurity part  $H_{\text{impurity}} = \epsilon_d d^\dagger d + it_M (d + d^\dagger) \gamma_1 / \sqrt{2}$ , where  $d$  indicates the dot that couples to one MZM  $\gamma_1$ . The other MZM  $\gamma_2$  [not shown in Fig. 1(a)] decouples from  $\gamma_1$ , to enforce the degeneracy between topological parities. For later convenience, we define an auxiliary fermionic operator  $d_{\text{MZM}} \equiv (\gamma_1 - i\gamma_2) / \sqrt{2}$  with MZMs. The lead Hamiltonian  $H_{\text{leads}}$  contains two free fermionic leads, and bosonic environ-

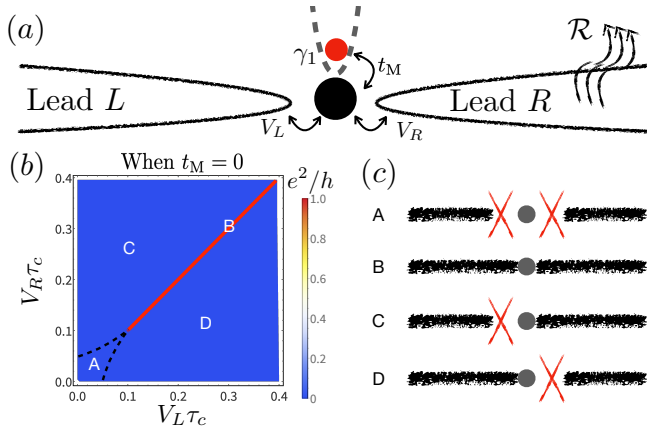


Figure 1. (a) The model of the system. The MZM (the red dot) couples to the dot of the DRLM, with the amplitude  $t_M$ . The dot couples to two leads with corresponding dimensionless tunneling amplitudes  $V_L \tau_c$  and  $V_R \tau_c$ , with  $\tau_c$  the cutoff in imaginary time. The leads are dissipative, with the *total* impedance  $\mathcal{R}$ . When  $t_M = 0$ , the system reduces to the DRLM, with the zero-temperature equilibrium conductance in (b) (when  $r = 2.5$ ). The marked-out phases A, B, C and D are illustrated in (c), with red crosses indicating vanishing lead-dot communications.

mental modes. With those modes included, the lead-impurity tunneling Hamiltonian  $H_T = V_L \psi_L^\dagger d e^{i\varphi_L} + V_R \psi_R^\dagger d e^{i\varphi_R} + h.c.$  contains the dynamical phase  $\varphi_\alpha$  that is conjugate to the charge number  $N_\alpha = \int dx \psi_\alpha^\dagger(x) \psi_\alpha(x)$ , in the corresponding lead  $\alpha = L, R$ . After integrating out the environmental modes,  $\varphi_L = -\varphi_R = \varphi$ , with the long-time dynamical feature  $\langle \varphi(\tau) \varphi(0) \rangle \sim 2r \ln \tau$  [29], where  $r = \mathcal{R} e^2/h$  is the ratio between the Ohmic impedance  $\mathcal{R}$  of the dissipative leads, and the resistance quanta  $h/e^2$ . The required dissipation has been realized in real experiments [10, 11, 30, 31]. Finally, two leads couple to the dot, with hybridization parameters  $V_L$  and  $V_R$ .

Dissipative modes introduce effective many-body interaction to the system [32–34]. We then bosonize lead fermions after extending semi-infinite leads into chiral full-1D ones [35, 36]  $\psi_\alpha(x) = F_\alpha \exp[i\phi_\alpha(x)]/\sqrt{2\pi a}$ , where  $a$  is the short-distance cutoff, and  $F_\alpha$  is the Klein factor that enforces the fermionic anti-commutator. Finally, the bosonic phase  $\phi_\alpha$  satisfies the commutation relation  $[\phi_\alpha(x), \phi_{\alpha'}(x')] = i\pi\Theta(x - x')\delta_{\alpha, \alpha'}$ . These fields are related to the charge numbers in two leads  $N_{L,R} = e[\phi_{L,R}(\infty) - \phi_{L,R}(-\infty)]/(2\pi)$ . To proceed, we define the common and difference fields with the rotation  $\phi_{c,f} = (\phi_L \pm \phi_R)/\sqrt{2}$ . The post-rotation fields  $\phi_c$  and  $\phi_f$  reflect the total charge number  $N_L + N_R$ , and the number difference  $N_L - N_R$ , respectively. With bosonization and the rotation, the dissipative phase can be combined with the difference field  $\phi'_f \equiv (\phi_f + \varphi/\sqrt{2})/\sqrt{1+r}$ . The addressed dissipative phase  $\varphi' \equiv (\sqrt{r}\phi_f - \varphi/\sqrt{2r})/\sqrt{1+r}$  decouples, reducing the system degrees of freedom.

**BKT QPT of the DRLM** — When the MZM decouples ( $t_M = 0$ ), the system reduces to the regular DRLM, where a boundary BKT QPT is predicted [12] when  $2 < r < 3$  and  $V_L = V_R$  [37] (see an alternative QPT interpreta-

tion in Ref. [20]). When  $V_L = V_R$  is larger than a critical value [38], the system flows to the ballistic-transmission phase with conductance  $e^2/h$  [Line B in the phase diagram of Fig. 1(b)]. Notice that this conductance is different from that of Ref. [39, 40], due to the dissipative and interacting effect [10, 41–46]. By contrast, with couplings smaller than the critical value, the system instead flows to the isolated-impurity phase [A of Fig. 1(b)] with zero conductance. The transition (between phases A and B) is of BKT-type, due to the absence of QCP. Indeed, it shares equivalent scaling equations as that of an XY-model, the pioneering model of topological transition [47–49]. More specifically, when  $r > 2$ , the lead-dot coupling is originally RG irrelevant [i.e., with scaling dimension larger than one [50], see Eq. (2)]. The couplings then, initially, decrease during the RG flow. If  $V_L = V_R$  are initially large enough, the dot charge number gradually becomes fixed at half-filling [12, 35]. The common field, reflecting the charge number fluctuation, then loses its scaling dimension after the RG, leading to a relevant lead-dot coupling if  $r < 3$ . Briefly, the change of scaling dimension (upon the RG flow) leads to the BKT QPT: the system can enter the ballistic-transmission phase, only if  $V_L$  and  $V_R$  become relevant before they vanish; otherwise the flow terminates in the isolated-impurity phase.

Importantly, this BKT QPT requires a strict left-right symmetry  $V_L = V_R$ . Indeed, if  $V_L \neq V_R$ , the system flows to other two zero-conductance phases [C and D of Fig. 1(b)]. The transition  $C \leftrightarrow B \leftrightarrow D$ , with state B as the QCP, is not of BKT type. As our main result, we show that with a finite Majorana-dot coupling  $t_M$ , the strict left-right symmetry to observe the BKT QPT is relaxed. Indeed, as shown in Fig. 2, the ballistic-transmission phase (area B) has extended from a 1D line [Fig. 1(b)] to a 2D space. The specific phase diagram changes under the different values of  $t_M$ : when  $t_M$  decreases [i.e. increasing cutoff  $l_C$ , from Fig. 2(a) to Fig. 2(b)], the ballistic-transmission phase requires a smaller lead-dot tunnelings, but has a worse tolerance against left-right asymmetry.

**Coulomb gas RG** — In this work, we obtain the phase diagram of Fig. 2 (a,b) with the method of Coulomb gas RG [35, 51]. Briefly, within the Coulomb gas representation, one works with the partition function

$$\mathcal{Z} = \sum_n \int_0^{1/T} d\tau_1 \cdots \int_0^{\tau_1 - \tau_c} d\tau_{i+1} \cdots \int_0^{\tau_{n-1} - \tau_c} d\tau_n \quad (1)$$

$$\langle H_T(\tau_1) \cdots H_T(\tau_{i+1}) \cdots H_T(\tau_n) \rangle_{H_{\text{leads}} + H_{\text{impurity}}},$$

where  $n$  refers to the number of lead-impurity tunneling events during imaginary time  $1/T$ , and  $\tau_c$  is the cutoff: for any  $i \in [1, n-1]$ ,  $\tau_i - \tau_{i+1} > \tau_c$  is enforced. Expansions of Eq. (1) are carried out within the interaction picture [52], over lead-impurity tunnelings  $H_T$ . One can perform RG calculations [35] as follows. During each RG step, one starts with the cutoff  $\tau_c$ , and increases it to  $\tau_c + d\tau_c$  (indicating the temperature decreasing). The pairs of tunneling events at  $\{\tau_i, \tau_{i+1}\}$  with condition  $\tau_c < |\tau_i - \tau_{i+1}| < \tau_c + d\tau_c$  should be integrated out. RG flow equations are then obtained, af-

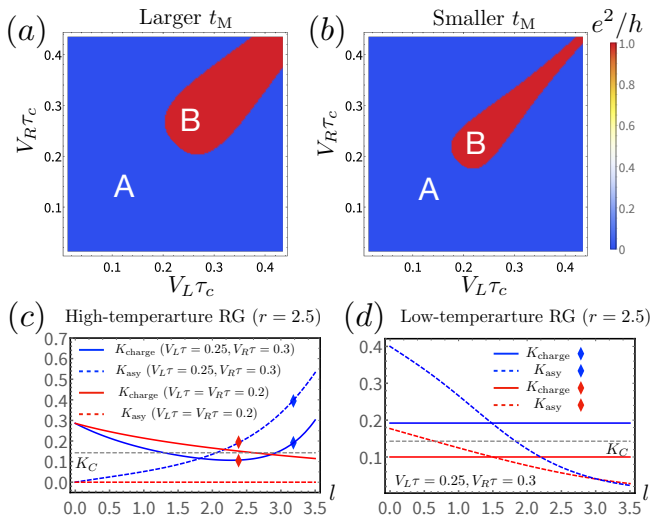


Figure 2. Phase diagrams (indicated by the corresponding zero-temperature equilibrium conductance) and RG flow curves when  $r = 2.5$ . (a), (b) are the phase diagrams with  $l_C = 2$  and  $l_C = 3$ , respectively, with the corresponding  $t_M$  ratio 1 : 0.37. (c) High-temperature RG flows curves of  $K_{\text{charge}}$  and  $K_{\text{asy}}$ , for the symmetric (red curves) and asymmetric (blue curves) situations. The red and blue diamonds marked out points that belong to the ballistic-transmission ( $K_{\text{charge}} < K_C$ ) and isolated-impurity ( $K_{\text{charge}} > K_C$ ) phases, respectively, if high-temperature RG flow terminates at their corresponding  $l$ . (d) Low-temperature RG flow of  $K_{\text{charge}}$  and  $K_{\text{asy}}$ , with their initial values given by the corresponding diamond.

ter rescaling the cutoff, and enforcing the invariance of  $\mathcal{Z}$ . In Eq. (1), the correlator of  $H_T$  equals the product of the free-lead correlation (with the environmental modes included) and the impurity correlation. The free-lead contribution can be straightforwardly obtained [12, 35].

The impurity correlator can be obtained by solving the Hamiltonian  $H_{\text{impurity}}$ , leading to four impurity eigenstates: two even-parity ones  $|\psi_{1,3}\rangle = \frac{1}{\sqrt{2}}(\mp i|1, 1\rangle + |0, 0\rangle)$ , and two odd-parity ones  $|\psi_{2,4}\rangle = \frac{1}{\sqrt{2}}(\mp i|1, 0\rangle + |0, 1\rangle)$ , where  $|n, m\rangle$  indicates the state with  $n$  and  $m$  particle (either 0 or 1) in the dot and the auxiliary dot  $d_{\text{MZM}}$ , respectively. Assuming  $t_M > 0$ , states  $|\psi_1\rangle$  and  $|\psi_2\rangle$  become the degenerate ground states: they have the energy  $-t_M$ , lower than that ( $t_M$ ) of  $|\psi_3\rangle$  and  $|\psi_4\rangle$ .

Without lead-dot tunneling, the impurity part stays in two possible ground states  $|\psi_1\rangle$  and  $|\psi_2\rangle$ . After one lead-dot tunneling, they become  $d|\psi_1\rangle = -\frac{i}{2}(|\psi_2\rangle + |\psi_4\rangle)$ ,  $d^\dagger|\psi_1\rangle = \frac{i}{2}(|\psi_2\rangle - |\psi_4\rangle)$ ,  $d|\psi_2\rangle = -\frac{i}{2}(|\psi_1\rangle + |\psi_3\rangle)$ , and  $d^\dagger|\psi_2\rangle = \frac{i}{2}(|\psi_1\rangle - |\psi_3\rangle)$ , resulting in (non-eigen) final states with impurity parities different from the initial ones. The impurity state before the next lead-impurity tunneling depends on the evolution time [38]. For the low-temperature limit  $T \ll t_M$ , tunnelings are rare, the impurity state evolves back to the ground states  $|\psi_1\rangle$  and  $|\psi_2\rangle$  before the next tunneling. By contrast, for the high-temperature situation  $T \gg t_M$ , lead-dot tunnelings are frequent, and the impurity state stays in the non-eigenstate before the next lead-impurity tunneling. We thus

have to treat the low-temperature and high-temperature situations separately.

**The high-temperature RG flow** — We start by visiting the high-temperature regime  $T \gg t_M$ , where all four impurity states are energetically allowed. Of this case, the impurity-lead tunneling histories with alternating creation and annihilation operators dominate the partition function [38]. The effect of the MZM-dot coupling is then negligible, leading to RG equations that approximately equal that of a normal DRLM (following Ref. [12], or reducing Luttinger liquid spinful results of Ref. [53] to the spinless case),

$$\begin{aligned} dV_{L,R}/dl &= V_{L,R} \left[ 1 - \frac{1+r}{4} (1 + K_{\text{charge}} \pm 2K_{\text{asy}}) \right], \\ dK_{\text{charge}}/dl &= -4\tau_c^2 [K_{\text{charge}}(V_L^2 + V_R^2) + K_{\text{asy}}(V_L^2 - V_R^2)], \\ dK_{\text{asy}}/dl &= -2\tau_c^2 [K_{\text{asy}}(V_L^2 + V_R^2) + (V_L^2 - V_R^2)], \end{aligned} \quad (2)$$

where parameter  $l$  indicates the RG flow progress: it increases when temperature  $T$  decreases  $l \sim \ln(T_0/T)$ , with  $T_0$  the initial temperature (a device-dependent parameter that can only be characterized experimentally).  $K_{\text{charge}}$ , with its initial value  $1/(1+r)$ , refers to the scaling dimension of the common field  $\phi_c$ .  $K_{\text{asy}}$ , which equals zero initially, refers to the scaling dimension from the left-right asymmetry [12, 35]. For the symmetric case  $V_L = V_R$ ,  $K_{\text{asy}}$  is fixed at zero [red dashed line of Fig. 2(c)]. The scaling dimension of lead-dot tunnelings becomes smaller than one (thus RG relevant) when  $K_{\text{charge}}$  has become smaller than  $K_C = 4/(1+r) - 1$ . For asymmetric situations, by contrast,  $|K_{\text{asy}}|$  increases during the RG flow [blue dashed line of Fig. 2(c)], after which the larger lead-dot coupling becomes more relevant than the weaker one, leading to an even more significant asymmetry [38]. The high-temperature flow terminates when  $T \sim t_M$ .

**Low-temperature RG, and the phase diagram** — For the low-temperature case  $T \ll t_M$ , only ground states are allowed as real states in the impurity, and after one lead-dot tunneling, the impurity system prefers to evolve to one of the ground states ( $|\psi_1\rangle$  or  $|\psi_2\rangle$ ), before the next lead-dot tunneling event. Neighbouring dot operators can be thus the same: a consequence of the presence of topological degeneracy. Low-temperature RG equations of an MZM-involved system become [38]

$$\begin{aligned} dV_{L,R}/dl &= V_{L,R} \left[ 1 - \frac{1+r}{4} (1 + K_{\text{charge}} \pm 2K_{\text{asy}}) \right], \\ dK_{\text{charge}}/dl &= 0, \quad dK_{\text{asy}}/dl = -2\tau_c^2 (V_L^2 + V_R^2) K_{\text{asy}}, \end{aligned} \quad (3)$$

with initial values of  $K_{\text{charge}}$  and  $K_{\text{asy}}$ , importantly, inherited from the RG-flow of the previous stage. The low-temperature flow Eq. (3) contains two major Majorana-induced modifications: (i)  $K_{\text{charge}}$ , which initially decreases in the high-temperature situation [solid lines of Fig. 2(c)], now stops flowing [solid lines of Fig. 2(d)], and, more importantly, (ii)  $K_{\text{asy}}$ , which increases in the asymmetric case of the high-temperature limit [dashed red line of Fig. 2(c)], now instead begins to decrease to zero [dashed lines of Fig. 2(d)]. Modification (ii), remarkably, is the key element that leads to the

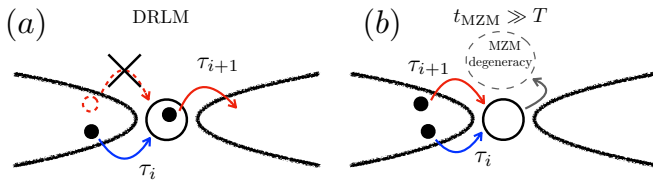


Figure 3. Lead-impurity tunneling events. (a) In a regular DRLM, the dot state alternates in time. (b) In great contrast, with tunneling into the MZM degeneracy (the grey arrow), two neighbouring dot-lead tunneling events (shown by the blue and red arrows) can both contain a creation operator in the dot.

irrelevance of a weak asymmetry. Indeed, when  $K_{\text{asy}}$  has vanished,  $dV_{L,R}/dl = V_{L,R} [1 - (1+r)(1+K_{\text{charge}})/4]$ , where  $V_L$  and  $V_R$  simultaneously increase to perfect or decrease to zero, disregarding a weak asymmetry. Noticeably, the irrelevance of asymmetry also removes phases C and D in Fig. 1(c), where only one lead-impurity coupling (the smaller one of  $V_L$  or  $V_R$ ) flows to zero. As the consequence of (i), the final phase is determined by the value of  $K_{\text{charge}}$ , larger or smaller than  $K_C$ , at the end of high-temperature flow [as shown in Fig. 2(d)].

One can physically understand these two modifications with Fig. 3. Briefly, in DRLM [with corresponding RG equations (2)] the dot state alternates in time [Fig. 3(a)], where  $N_L + N_R$  has only two possible (integer) options. Field  $\phi_c$ , reflecting fluctuations of  $N_L + N_R$ , then gradually loses its scaling dimension [reflected by the decreasing  $K_{\text{charge}}$  of Eq. (2)] when  $N_L + N_R$  is fixed by a half-filling dot [35]. In great contrast, with Majorana involved, the parity of the impurity part, including the dot and a coupled MZM, alternates in time [Fig. 3(b)]. The corresponding common field  $\phi_c$  now becomes a free 1D field. Its scaling dimension  $K_{\text{charge}}$  thus remains invariant during RG flow of Eq. (3). We emphasize, importantly, the necessity of topological degeneracy in the picture above. Indeed, if the DRLM dot couples to a zero-energy Andreev bound state, the impurity part has a unique ground state (instead of two degenerate ground states of the MZM situation). This case reduces to the DRLM with a detuned dot [38]: a system with only the isolated-impurity phase [10–12].

Modifications above also explain features of Fig. 2(a, b). More specifically, with a larger  $t_M$  of Fig. 2(a), (i) for the symmetric case, a larger value of  $V_L = V_R$  is required to enter the ballistic-transmission phase, and (ii) for the asymmetric case, the ballistic-transmission phase tolerates a larger value of  $V_L - V_R$ . Feature (i) is a consequence of an earlier termination, due to a larger  $t_M$ , of the high-temperature flow. Feature (ii) is related to the non-monotonous curve of  $K_{\text{charge}}$  [blue solid line of Fig. 2(c)].

**Discussions** — In this paper, we show that the MZM-introduced topological degeneracy can relax the strict symmetry requirement  $V_L = V_R$  for a BKT QPT in a DRLM. This result can be understood with the g-theorem [27, 28], by visiting the effect of a weak asymmetry in the strong tunneling regime. Briefly, the g-theorem claims that in a boundary

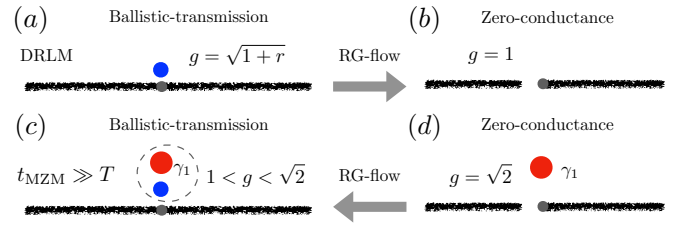


Figure 4. The effect of left-right asymmetry (assuming  $V_L < V_R$ ) in a regular [(a) and (b)] and Majorana-involved DRLM [(c) and (d)]. The red and blue dots refer to the MZM and the residue degeneracy ( $g = \sqrt{1+r}$ ) of the ballistic-transmission phase, respectively. The grey dot instead indicates the hybridized dot degree of freedom. RG flow prefers the fixed point with a smaller degeneracy.

QPT, the phase with a smaller degeneracy is more stable. Indeed, in a regular asymmetry-present DRLM, the fixed point where the dot is fully hybridized by the stronger lead has a smaller degeneracy [degeneracy  $g = 1$ , in Fig. 4(b)] than that of the ballistic-transmission fixed point [ $g = \sqrt{1+r}$  [54], Fig. 4(a)]. The zero-conductance phase is thus more stable, in a regular DRLM. With the Majorana-parity provided, the fixed point where dot is hybridized by the stronger lead has the degeneracy  $\sqrt{2}$  [Fig. 4(d)], the degeneracy of a single MZM: larger than that [Fig. 4(b)] of the MZM absent situation. For the ballistic transmission case, the Majorana couples to the residued dot-degeneracy (i.e.,  $\sqrt{1+r}$ ). The degeneracy of the impurity part, obtained after the MZM-residue fusion [55, 56] (see e.g., Ref. [57] as a pioneering work that applies fusion rules to boundary QPT studies), is generally hard to obtain. Indeed, an arbitrary  $r$  does not necessarily correspond to a discrete Virasoro algebra with central charge  $c < 1$  [55]. We can however evaluate the possible range of degeneracy, with fusion between primary fields of the Ising model ( $c = 1/2$ ). Indeed, if  $r = 1$ , we have the fusion  $[\sqrt{1+r}] \times [\sqrt{2}] = [\sqrt{2}] \times [\sqrt{2}] = [1] + [2]$ , with numbers indicating the degeneracy. For  $r = 3$ , instead  $[\sqrt{1+r}] \times [\sqrt{2}] = [2] \times [\sqrt{2}] = [\sqrt{2}] + [2\sqrt{2}]$ . Taking the smaller degeneracy of both cases, the Majorana-involved ballistic-transmission phase thus has a smaller degeneracy [ $1 < g < \sqrt{2}$ , Fig. 4(c)] than that ( $\sqrt{2}$ ) of the zero-conductance one, indicating a stabilized ballistic-transmission phase against a weak asymmetry. Importantly, similar g-theorem analysis applies to situations with a finite  $\epsilon_d$ : the BKT QPT thus tolerates also a small dot detuning [38].

Before closure, we emphasize that the predicted significant MZM-induced modification of the BKT QPT phase diagram can also signify the Majorana existence, in a much more convincing way than the quantized plateau, as our proposal detects the non-trivial degeneracy of an MZM. Encouraged by persistent progress of Majorana hunting in nanodevices [58–67], especially for the cases with dissipative environments [68–72], we anticipate the experimental capability to observe our predicted phenomenon. Prospectively, QPTs are also potentially capable to identify Majorana non-localities [73–78], another crucial elements in topological

quantum device.

*Acknowledgements.*— The authors thank Hao Zhang for valuable discussions. This work was supported by the Innovation Program for Quantum Science and Technology (Grant No. 2021ZD0302400), the National Natural Science Foundation of China (Grants No. 11974198 and No. 12004040).

\* zhanggu@baqis.ac.cn

† dongeliu@mail.tsinghua.edu.cn

- [1] M. Vojta, *Philosophical Magazine* **86**, 1807 (2006), <https://doi.org/10.1080/14786430500070396>.
- [2] I. Affleck, “Quantum impurity problems in condensed matter physics,” (2008).
- [3] V. J. Emery and S. Kivelson, *Phys. Rev. B* **46**, 10812 (1992).
- [4] I. Affleck and A. W. Ludwig, *Nuclear Physics B* **360**, 641 (1991).
- [5] I. Affleck and A. W. W. Ludwig, *Phys. Rev. Lett.* **68**, 1046 (1992).
- [6] I. Affleck, A. W. W. Ludwig, H.-B. Pang, and D. L. Cox, *Phys. Rev. B* **45**, 7918 (1992).
- [7] A. K. Mitchell, L. A. Landau, L. Fritz, and E. Sela, *Phys. Rev. Lett.* **116**, 157202 (2016).
- [8] P. L. S. Lopes, I. Affleck, and E. Sela, *Phys. Rev. B* **101**, 085141 (2020).
- [9] A. Komnik and A. O. Gogolin, *Phys. Rev. Lett.* **90**, 246403 (2003).
- [10] H. T. Mebrahtu, I. V. Borzenets, D. E. Liu, H. Zheng, Y. V. Bomze, A. I. Smirnov, H. U. Baranger, and G. Finkelstein, *Nature* **488**, 61 (2012).
- [11] H. T. Mebrahtu, I. V. Borzenets, H. Zheng, Y. V. Bomze, A. I. Smirnov, S. Florens, H. U. Baranger, and G. Finkelstein, *Nat. Phys.* **9**, 732 (2013).
- [12] D. E. Liu, H. Zheng, G. Finkelstein, and H. U. Baranger, *Phys. Rev. B* **89**, 085116 (2014).
- [13] S. Sachdev, *Quantum Phase Transitions*, 2nd ed. (Cambridge University Press, 2011).
- [14] E. Cornfeld, L. A. Landau, K. Shtengel, and E. Sela, *Phys. Rev. B* **99**, 115429 (2019).
- [15] P. L. S. Lopes, I. Affleck, and E. Sela, *Phys. Rev. B* **101**, 085141 (2020).
- [16] Y. Komijani, *Phys. Rev. B* **101**, 235131 (2020).
- [17] M. Lotem, E. Sela, and M. Goldstein, *Phys. Rev. Lett.* **129**, 227703 (2022).
- [18] D. Gabay, C. Han, P. L. S. Lopes, I. Affleck, and E. Sela, *Phys. Rev. B* **105**, 035151 (2022).
- [19] G. Zhang and C. Spånslätt, *Phys. Rev. B* **102**, 045111 (2020).
- [20] C.-H. Chung, K. Le Hur, M. Vojta, and P. Wölfle, *Phys. Rev. Lett.* **102**, 216803 (2009).
- [21] A. Y. Kitaev, **44**, 131 (2001).
- [22] R. M. Lutchyn, J. D. Sau, and S. Das Sarma, *Phys. Rev. Lett.* **105**, 077001 (2010).
- [23] Y. Oreg, G. Refael, and F. von Oppen, *Phys. Rev. Lett.* **105**, 177002 (2010).
- [24] N. Read and D. Green, *Phys. Rev. B* **61**, 10267 (2000).
- [25] L. Fu and C. L. Kane, *Phys. Rev. Lett.* **100**, 096407 (2008).
- [26] C. Nayak, S. H. Simon, A. Stern, M. Freedman, and S. Das Sarma, *Rev. Mod. Phys.* **80**, 1083 (2008).
- [27] I. Affleck and A. W. Ludwig, *Phys. Rev. Lett.* **67**, 161 (1991).
- [28] I. Affleck and A. W. W. Ludwig, *Phys. Rev. B* **48**, 7297 (1993).
- [29] G.-L. Ingold and Y. V. Nazarov, “Charge tunneling rates in ultrasmall junctions,” in *Single Charge Tunneling: Coulomb Blockade Phenomena In Nanostructures*, edited by H. Grabert and M. H. Devoret (Springer US, Boston, MA, 1992) pp. 21–107.
- [30] F. D. Parmentier, A. Anthore, S. Jezouin, H. le Sueur, U. Gennser, A. Cavanna, D. Mailly, and F. Pierre, *Nature Physics* **7**, 935 (2011).
- [31] S. Jezouin, M. Albert, F. D. Parmentier, A. Anthore, U. Gennser, A. Cavanna, I. Safi, and F. Pierre, *Nat. Commun.* **4**, 1802 (2013).
- [32] Y. V. Nazarov, *Sov. Phys. JETP* **68**, 561 (1989).
- [33] I. Safi and H. Saleur, *Phys. Rev. Lett.* **93**, 126602 (2004).
- [34] S. Florens, P. Simon, S. Andergassen, and D. Feinberg, *Phys. Rev. B* **75**, 155321 (2007).
- [35] C. L. Kane and M. P. A. Fisher, *Phys. Rev. B* **46**, 15233 (1992).
- [36] T. Giamarchi, *Quantum Physics in One Dimension* (Oxford Univ. Press, Oxford UK, 2004).
- [37] The QPT is not of BKT-type when  $r < 2$  [10]. When  $r > 3$ , the dot is always isolated.
- [38] See Supplemental Material for more details.
- [39] D. E. Liu and H. U. Baranger, *Phys. Rev. B* **84**, 201308 (2011).
- [40] E. Vernek, P. H. Penteado, A. C. Seridonio, and J. C. Egues, *Phys. Rev. B* **89**, 165314 (2014).
- [41] I. Safi and H. J. Schulz, *Phys. Rev. B* **52**, R17040 (1995).
- [42] D. L. Maslov and M. Stone, *Phys. Rev. B* **52**, R5539 (1995).
- [43] V. V. Ponomarenko, *Phys. Rev. B* **52**, R8666 (1995).
- [44] A. Kawabata, *Journal of the Physical Society of Japan* **65**, 30 (1996), <https://doi.org/10.1143/JPSJ.65.30>.
- [45] C. de C. Chamon and E. Fradkin, *Phys. Rev. B* **56**, 2012 (1997).
- [46] Y. Hu and C. L. Kane, “Universal symmetry-protected resonances in a spinful luttinger liquid,” (2016), arXiv:1604.08280.
- [47] V. Berezinskii, *Sov. Phys. JETP* **32**, 493 (1971).
- [48] J. Kosterlitz, *Journal of Physics C: Solid State Physics* **7**, 1046 (1974).
- [49] J. M. Kosterlitz and D. J. Thouless, in *Basic Notions Of Condensed Matter Physics* (CRC Press, 2018) pp. 493–515.
- [50] A. Altland and B. D. Simons, *Condensed Matter Field Theory*, 2nd ed. (Cambridge University Press, 2010).
- [51] P. W. Anderson, G. Yuval, and D. R. Hamann, *Phys. Rev. B* **1**, 4464 (1970).
- [52] H. Bruus and K. Flensberg, *Many-body quantum theory in condensed matter physics - an introduction* (Oxford University Press, United States, 2004).
- [53] A. Schiller and K. Ingersent, *Europhysics Letters* **39**, 645 (1997).
- [54] H. Zheng, S. Florens, and H. U. Baranger, *Phys. Rev. B* **89**, 235135 (2014).
- [55] P. Ginsparg, arXiv preprint hep-th/9108028 (1988).
- [56] P. D. Francesco, P. Mathieu, and D. Sénéchal, *Condensed Matter Field Theory*, 1st ed. (Springer, 1997).
- [57] I. Affleck, A. W. W. Ludwig, and B. A. Jones, *Phys. Rev. B* **52**, 9528 (1995).
- [58] V. Mourik, K. Zuo, S. M. Frolov, S. Plissard, E. P. Bakkers, and L. P. Kouwenhoven, *Science* **336**, 1003 (2012).
- [59] M. T. Deng, S. Vaitiekėnas, E. B. Hansen, J. Danon, M. Leijnse, K. Flensberg, J. Nygård, P. Krogstrup, and C. M. Marcus, *Science* **354**, 1557 (2016).
- [60] S. M. Albrecht, A. P. Higginbotham, M. Madsen, F. Kuemmeth, T. S. Jaspersen, J. Nygård, P. Krogstrup, and C. M. Marcus, *Nature* **531**, 206 (2016).
- [61] A. Fornieri, A. M. Whiticar, F. Setiawan, E. Portolés, A. C. Drachmann, A. Keselman, S. Gronin, C. Thomas, T. Wang, R. Kallaher, *et al.*, *Nature* **569**, 89 (2019).
- [62] H. Ren, F. Pientka, S. Hart, A. T. Pierce, M. Kosowsky, L. Lunczer, R. Schlereth, B. Scharf, E. M. Hankiewicz, L. W.

- Molenkamp, *et al.*, *Nature* **569**, 93 (2019).
- [63] S. Vaitiekėnas, Y. Liu, P. Krogstrup, and C. Marcus, *Nat. Phys.* **17**, 43 (2021).
- [64] H. Song, Z. Zhang, D. Pan, D. Liu, Z. Wang, Z. Cao, L. Liu, L. Wen, D. Liao, R. Zhuo, D. E. Liu, R. Shang, J. Zhao, and H. Zhang, *Phys. Rev. Research* **4**, 033235 (2022).
- [65] Z. Wang, H. Song, D. Pan, Z. Zhang, W. Miao, R. Li, Z. Cao, G. Zhang, L. Liu, L. Wen, R. Zhuo, D. E. Liu, K. He, R. Shang, J. Zhao, and H. Zhang, *Phys. Rev. Lett.* **129**, 167702 (2022).
- [66] M. Aghaee, A. Akkala, Z. Alam, R. Ali, A. A. Ramirez, M. Andrzejczuk, A. E. Antipov, M. Astafev, B. Bauer, J. Becker, *et al.*, [arXiv:2207.02472](https://arxiv.org/abs/2207.02472) (2022).
- [67] T. Dvir, G. Wang, N. van Loo, C.-X. Liu, G. P. Mazur, A. Bordin, S. L. D. ten Haaf, J.-Y. Wang, D. van Driel, F. Zatelli, X. Li, F. K. Malinowski, S. Gazibegovic, G. Badawy, E. P. A. M. Bakkers, M. Wimmer, and L. P. Kouwenhoven, *Nature* **614**, 445 (2023).
- [68] D. E. Liu, *Phys. Rev. Lett.* **111**, 207003 (2013).
- [69] D. Liu, G. Zhang, Z. Cao, H. Zhang, and D. E. Liu, *Phys. Rev. Lett.* **128**, 076802 (2022).
- [70] S. Zhang, Z. Wang, D. Pan, H. Li, S. Lu, Z. Li, G. Zhang, D. Liu, Z. Cao, L. Liu, L. Wen, D. Liao, R. Zhuo, R. Shang, D. E. Liu, J. Zhao, and H. Zhang, *Phys. Rev. Lett.* **128**, 076803 (2022).
- [71] Z. Wang, S. Zhang, D. Pan, G. Zhang, Z. Xia, Z. Li, D. Liu, Z. Cao, L. Liu, L. Wen, D. Liao, R. Zhuo, Y. Li, D. E. Liu, R. Shang, J. Zhao, and H. Zhang, *Phys. Rev. B* **106**, 205421 (2022).
- [72] S. Zhang, Z. Wang, D. Pan, Z. Wang, Z. Li, Z. Zhang, Y. Gao, Z. Cao, G. Zhang, L. Liu, *et al.*, [arXiv:2211.07170](https://arxiv.org/abs/2211.07170) (2022).
- [73] G. W. Semenoff and P. Sodano, arXiv e-prints, cond-mat/0601261 (2006), [arXiv:cond-mat/0601261](https://arxiv.org/abs/cond-mat/0601261) [cond-mat.other].
- [74] L. Fu, *Phys. Rev. Lett.* **104**, 056402 (2010).
- [75] B. Béri and N. R. Cooper, *Phys. Rev. Lett.* **109**, 156803 (2012).
- [76] A. Altland and R. Egger, *Phys. Rev. Lett.* **110**, 196401 (2013).
- [77] B. Béri, *Phys. Rev. Lett.* **110**, 216803 (2013).
- [78] Y. Hao, G. Zhang, D. Liu, and D. E. Liu, *Nature Communications* **13**, 6699 (2022).
-

# Supplementary Information for “Influence of Majorana-parity degeneracy on the boundary Berezinskii-Kosterlitz-Thouless quantum phase transition of a dissipative resonant level”

Gu Zhang, Zhan Cao, and Dong E. Liu  
(Dated: March 20, 2023)

In this Supplementary Information, we provide details on: (i) RG equations and descriptions of BKT QPT in a regular DRLM, (ii) Correlation function of the impurity part, (iii) derivations of RG equations in the low-temperature regime, (iv) RG flow equations in the presence of a finite detuning of the dot ( $\epsilon_d$ ), and (v) the situation that the DRLM dot couples to a topologically trivial Andreev bound state.

## I. BKT TRANSITION IN DRLM

In this section, we provide more details to present the existence of a BKT QPT in DRLM. We start with the DRLM RG flow equation, Eq. (5) of the main text,

$$\begin{aligned}\frac{dV_{L,R}}{dl} &= V_{L,R} \left[ 1 - \frac{1+r}{4} (1 + K_{\text{charge}} \pm 2K_{\text{asy}}) \right], \\ \frac{dK_{\text{charge}}}{dl} &= -4\tau_c^2 [K_{\text{charge}}(V_L^2 + V_R^2) + K_{\text{asy}}(V_L^2 - V_R^2)], \\ \frac{dK_{\text{asy}}}{dl} &= -2\tau_c^2 [K_{\text{asy}}(V_L^2 + V_R^2) + (V_L^2 - V_R^2)].\end{aligned}\tag{S1}$$

Without the Majorana, the flow of Eq. (S1) continues until arriving at the cutoff: either temperature of bias. For the symmetric case  $V_L = V_R$ , we obtain the flow of  $K_{\text{charge}}$  in Fig. S1(a). Here the dashed and solid red lines have  $V_L = V_R = 0.095/\tau_c$  and  $V_L = V_R = 0.1/\tau_c$ , respectively. The dashed grey line indicates the critical value [ $K_C = 4/(1+r) - 1$ ] of  $K_{\text{charge}}$ : lead-dot tunnelings become relevant when  $K_{\text{charge}} < K_C$ , and irrelevant given the opposite situation, i.e.,  $K_{\text{charge}} > K_C$ . If  $K_{\text{charge}} > K_C$  during the entire RG flow [the red dashed line of Fig. S1(a)], couplings of the dot to both leads are always irrelevant, and the system flows to the isolated-impurity phase with zero equilibrium conductance. By contrast, if  $K_{\text{charge}} < K_C$  after the RG flow [the red solid line of Fig. S1(a)], system flows instead to the ballistic-transmission phase with perfect conductance  $e^2/h$ . Analysis above leads to the RG flow diagram of Ref. [S1] (one can see Ref. [S2] for an alternative interpretation of this BKT QPT), shown in Fig. S1(b).

Now we move to discuss the influence of asymmetry. Figs. S1(c) and S1(d) present the flow of dot-lead couplings and scaling parameters ( $K_{\text{charge}}$  and  $K_{\text{asy}}$ ), respectively. As the stronger lead-dot tunneling,  $V_L$  becomes RG relevant (i.e., increases with an increasing  $l$ ) after the flow. The weaker one however remains irrelevant. In (d), we further see that  $V_L$  becomes relevant when  $K_{\text{charge}} > K_C$ , due to a finite  $K_{\text{asy}}$ .

## II. CORRELATION FUNCTION OF THE IMPURITY PART

In this section we provide detailed discussions on the eigenstates of the impurity part, and the evolution of impurity states after lead-impurity tunnelings. As a reminder, in this work we consider the impurity Hamiltonian

$$H_{\text{impurity}} = \epsilon_d d^\dagger d + it_M (d + d^\dagger) \gamma_1 / \sqrt{2},\tag{S2}$$

with  $d$  and  $d^\dagger$  the dot operators, and  $\gamma_1$  representing for the Majorana. As has been shown in the main text, in this work we take the Coulomb gas RG method, and work in the interaction picture that contains expansions over lead-impurity tunnelings. The corresponding correlation functions then contain the free-lead part and the isolated impurity part. The former one is straightforward within the Luttinger liquid formalism [S4], while the latter one equals

$$\langle \Pi_{i=1}^n D(\epsilon_i, \tau_i) \rangle = 2 \Pi_{i=1}^{n-1} g_{\text{dot}}(\tau_i - \tau_{i+1}, \epsilon_i, \epsilon_{i+1}),\tag{S3}$$

where we have, for convenience, defined another dot operator  $D(\epsilon_i, \tau_i)$ : it equals  $d^\dagger(\tau_i)$  and  $d(\tau_i)$  if  $\epsilon = \pm 1$ , respectively. The green's function  $g_{\text{dot}}(\tau, \epsilon, \epsilon') = [\exp(t_M \tau) - \epsilon \epsilon' \exp(-t_M \tau)]/2$ : it equals  $\sinh(t_M \tau)$  if dot operators of two involved neighbouring kinks are both creation or annihilation operators (i.e.,  $\epsilon_i \epsilon_{i+1} = 1$ ); otherwise ( $\epsilon_i \epsilon_{i+1} = -1$ ) it equals  $\cosh(t_M \tau)$ . One

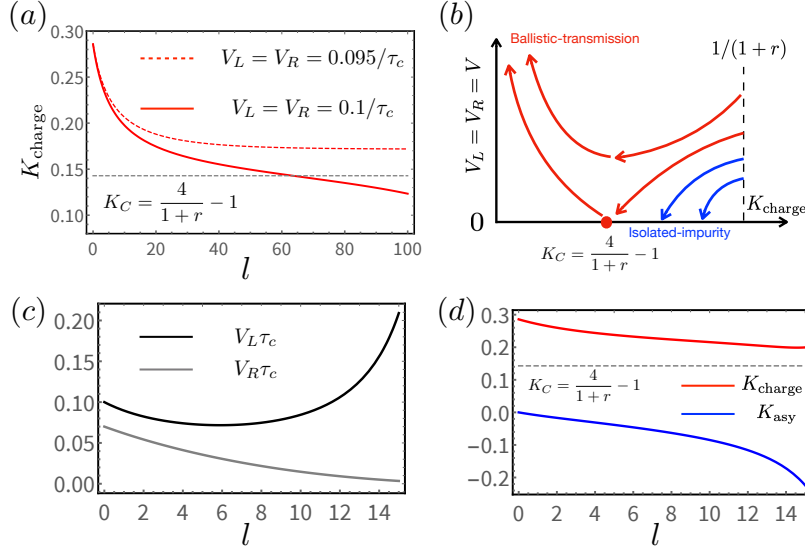


Figure S1. RG flows of a DRLM, when  $r = 2.5$ . (a) The flow of  $K_{\text{charge}}$ , when  $V_L = V_R = 0.095\tau_c$  (the dashed line) and  $V_L = V_R = 0.1\tau_c$  (the solid line), respectively. Of the latter case,  $K_{\text{charge}}$  flows beneath the critical value  $K_C = -1 + 4/(1+r)$ , leading to the ballistic-transmission phase. By contrast, of the former case,  $K_{\text{charge}}$  saturates to a value larger than  $K_C$ , leading to the isolated-impurity phase. (b) The corresponding RG flow diagram [S1]. It greatly mimics that of a Kondo model, where a BKT QPT is predicted between the fully screened and the isolated-impurity phases [S3]. (c) The flow of  $V_L$  and  $V_R$  if they start with different initial values.  $V_L$  becomes relevant (i.e., increases with an increasing  $l$ ) after the RG flow. The weaker one  $V_R$  however remains irrelevant. (d) The flow of  $K_{\text{charge}}$  and  $K_{\text{asy}}$ , with the same parameters in (c).  $V_L$  becomes relevant when  $K_{\text{charge}} > K_C$ , due to a finite  $K_{\text{asy}}$ .

can understand RG flows under different temperatures by visiting the corresponding features of Eq. (S3). Briefly, if temperature is large,  $\tau < 1/T \ll 1/t_M$ ,  $\sinh(t_M\tau) \ll \cosh(t_M\tau)$ , and lead-tunneling histories with alternating dot states (i.e., with  $\varepsilon_i \varepsilon_{i+1} = -1$ ) are preferred. The correlation function of the impurity part then greatly mimics that of a regular DRLM. By contrast, for a small temperature,  $\tau \gg 1/t_M$  in general,  $\sinh(t_M\tau) \approx \cosh(t_M\tau)$ , and now the parity of the entire impurity part alternates in time, leading to RG flows that are distinct from that of a regular DRLM.

One can similarly understand the difference between high-temperature and low-temperature situations, by looking into the time-dependent evolution of the impurity states. Without loss of generality, we assume the state  $|\psi_2\rangle = \frac{1}{\sqrt{2}}(-i|1,0\rangle + |0,1\rangle)$  of the impurity at a moment. After receiving one electron via a lead-impurity tunneling, impurity state becomes  $|1,1\rangle$ . As a non-eigen state,  $|1,1\rangle$  evolves in time, becoming  $\exp(-H_{\text{impurity}}\tau)|1,1\rangle = \cosh(t_M\tau)|1,1\rangle + i \sinh(t_M\tau)|0,0\rangle$ , after  $\tau$  of the tunneling. For the high-temperature limit, tunnelings are frequent,  $t_M\tau \ll 1$  is a small quantity. The impurity state  $\cosh(t_M\tau)|1,1\rangle + i \sinh(t_M\tau)|0,0\rangle \approx |1,1\rangle$  approximately equals that right after the lead-impurity tunneling. By contrast, for the low-temperature limit, tunnelings are rare,  $t_M\tau \gg 1$  is normally large. Of this case,  $\cosh(t_M\tau) \approx \sinh(t_M\tau)$ , and the impurity state approaches the ground state  $|\psi_1\rangle$ , which has an opposite parity from the initial one  $|\psi_2\rangle$ , before the next lead-dot tunneling. The RG flow is then distinct from that of a regular DRLM.

### III. LOW-TEMPERATURE RG FLOW EQUATIONS

In the section we provide detailed derivations of the low-temperature RG flow equations, Eq. (3) of the main text. Briefly, within the Coulomb-gas RG formalism, one deals with the partition function [S4]

$$Z = \sum_{\{q_j\}} \sum_{\{d_j\}} \prod_j t_j \left\langle \prod_j e^{i \frac{1}{\sqrt{2}} [q_j \phi_c(\tau_j) + d_j \phi_f(\tau_j)]} \right\rangle_{H_{\text{leads}}} \left\langle \prod_j D(\varepsilon_j, \tau_j) \right\rangle_{H_{\text{impurity}}} \quad (\text{S4})$$

for a two-lead system, where  $t_j = V_L, V_R$  refers to the amplitude of the  $j$ th tunneling event that occurs at time  $\tau_j$ . This tunneling event contains the impurity and lead operators  $D(\varepsilon_j, \tau_j)$  and  $\exp\left\{i \frac{1}{\sqrt{2}} [q_j \phi_c(\tau_j) + d_j \phi_f(\tau_j)]\right\}$ , respectively. Here  $q_j$  and  $d_j$  reflect the change of total lead charge ( $N_L + N_R$  of the main text), and the charge difference in two leads ( $N_L - N_R$  of the main text), respectively: they are charges considered in a regular DRLM [S1]. The dot operator  $D$  equals  $d^\dagger(\tau_i)$  and  $d(\tau_i)$  if  $\varepsilon = \pm 1$ , respectively.

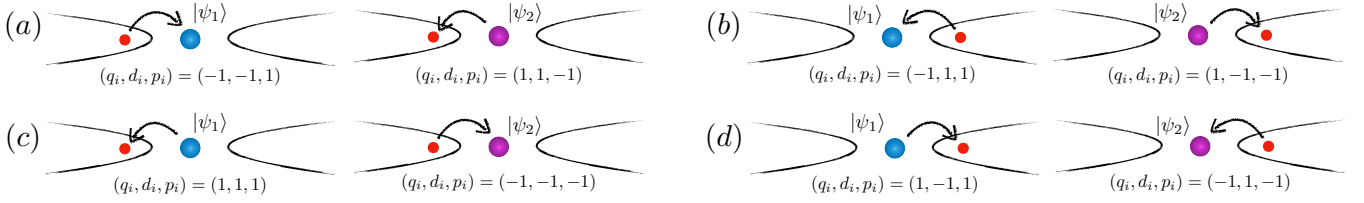


Figure S2. Four possible lead-impurity tunneling processes, of the  $i$ th tunneling. The cyan and purple dot refer to two different impurity ground states  $|\psi_1\rangle$  and  $|\psi_2\rangle$ , respectively. The red small dot refers to a tunneling electron. In each figure, the process at the right side is the inverse process of that at the left side. Charges  $q_i$  and  $d_i$  refer to the change of the total charge number, and the charge number differences in two leads, respectively. The third charge  $p_i$  refers to the change of parity of the impurity part.

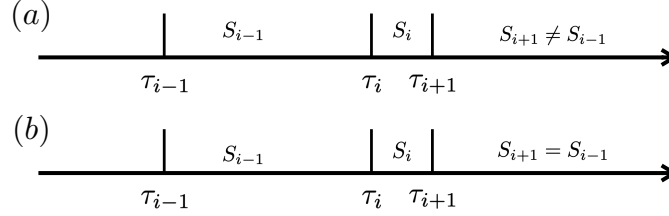


Figure S3. Two different pairs to deal with in Coulomb gas RG. (a) Of the non-neutral pair situation, the system state  $S_{i-1}$  before the close kink pairs (that occur at  $\tau_i$  and  $\tau_{i+1}$ , respectively) are different from that  $S_{i+1}$  after the pairs. One needs to combine non-neutral kinks at  $\tau_i$  and  $\tau_{i+1}$  into a single one. (b) When the pre and post-kink-pair states equal  $S_{i-1} = S_{i+1}$ , kinks at both  $\tau_i$  and  $\tau_{i+1}$  should be removed.

For the low-temperature situation,  $\sinh(\tau t_M) \approx \cosh(\tau t_M) \approx \exp(|\tau t_M|)$ . In addition, in this regime, the parity of the impurity part (instead of the dot occupation number of the high) alternates in time. We thus introduce another charge number, the parity charge  $p_j$ , to indicate the change of parity of the impurity part, before the  $j$ th tunneling event. The partition function then becomes

$$\mathcal{Z} = \sum_N \sum'_{\{q_j\}} \sum'_{\{d_j\}} \sum'_{\{p_j\}} \prod_{j=1}^N t_j \int_0^{\beta - \tau_c} d\tau_N \cdots \int_0^{\tau_{j+1} - \tau_c} d\tau_j \int_0^{\tau_j - \tau_c} d\tau_{j-1} \cdots \int_0^{\tau_2 - \tau_c} d\tau_1 e^{-\sum_{i < j} \mathcal{V}_{ij}} \prod_{j=1}^{N-1} e^{|\tau_j - \tau_{j+1}| t_M} \quad (\text{S5})$$

where prime indicates  $\sum_j q_j = \sum_j d_j = \sum_j p_j = 0$ , and the “potential interaction” equals

$$\mathcal{V}_{ij} = \frac{1+r}{2} \left[ \frac{1}{1+r} q_i q_j + d_i d_j + K_{\text{parity}} p_i p_j + K_{\text{asy}} (p_i d_j + p_j d_i) + \frac{1}{1+r} K'_{\text{asy}} (p_i q_j + p_j q_i) \right] \ln(\tau_i - \tau_j) / \tau_c, \quad (\text{S6})$$

where  $K_{\text{parity}}$  is the scaling factor of parity charge. Its initial value equals zero, since the lead fermion, after bosonization, contains only the common and different fields. Due to the alternating parity, another asymmetric scaling  $K'_{\text{asy}}$  is introduced, referring to the asymmetric scaling of the charge sector. It also has the initial value zero.

Following Eq. (S5), two neighbouring kinks are not allowed to occur within the time cutoff  $\tau_c$ . At the starting of each RG step, the cutoff increases to  $\tau_c + d\tau_c$ . Neighbouring kinks then have the chance to occur within the new cutoff, i.e.,  $\tau_c < |\tau_i - \tau_{i+1}| < \tau_c + d\tau_c$ . There are two different close kink pairs, as shown in Fig. S3. In Fig. S3(a), the state  $S_{i-1}$  and  $S_{i+1}$  are different, called as the non-neutral pair. Of this case, we can simply combine two kinks at  $\tau_i$  and  $\tau_{i+1}$ . Of the second case, in Fig. S3(b), these two states equal, known as the neutral pair. Of this case, both kinks need to be integrated out. In this work the BKT QPT occurs when transmissions are small. We thus ignore the non-neutral pairs. The inclusion of neutral pairs changes only the critical value of the coupling constant  $V_C$ , but not the qualitative feature.

The integral over neutral pair leads to the extra potential interaction  $\delta\mathcal{V}_{ij}$

$$\delta\mathcal{V}_{ij} = \sum_{\alpha} t_i^2 \frac{1+r}{2} \left[ \frac{1}{1+r} q_i q_j + d_i d_j + K_{\text{parity}} p_i p_j + K_{\text{asy}} (p_i d_j + p_j d_i) + \frac{1}{1+r} K'_{\text{asy}} (p_i q_j + p_j q_i) \right] \tau_c \partial_{\tau} \ln(\tau = \tau_j) / \tau_c, \quad (\text{S7})$$

after summation over all possible kink choices shown in Fig. S2. Notice that since the parity charge alternates in time,  $p = p_i$  is enforced, for all possible neutral pairs. One can then express other two charges of the neutral pair in terms of the parity charge.

After summing over all possible kinks, we arrive at extra potential generated from the neutral pair

$$\delta\mathcal{V}_j = -2(1+r)\tau_c(V_L^2 + V_R^2) [K_{\text{parity}}pp_j + K_{\text{asy}}pd_j + K'_{\text{asy}}pq_j] d\tau_c \ln(\tau_i - \tau). \quad (\text{S8})$$

The extra contribution above can be combined with other kinks, leading to the renormalization of scaling parameters

$$\frac{dK_{\text{parity}}}{dl} = -4\tau_c^2(V_L^2 + V_R^2)K_{\text{parity}}, \quad \frac{dK_{\text{asy}}}{dl} = -2\tau_c^2(V_L^2 + V_R^2)K_{\text{asy}}, \quad \frac{dK'_{\text{asy}}}{dl} = -2\tau_c^2(V_L^2 + V_R^2)K'_{\text{asy}}. \quad (\text{S9})$$

From Eq. (S9), we see that  $K_{\text{parity}}$  and  $K'_{\text{asy}}$ , with vanishing initial values, are both fixed at zero: the parity charge will not introduce extra asymmetric scaling parameters. In addition, although  $K_{\text{asy}}$  is finite at the end of the high-temperature flow, it gradually decreases to zero in the low-temperature flow. The asymmetry is thus irrelevant in the low-temperature regime.

#### IV. RG FLOW OF A FINITE DOT ENERGY $\epsilon_d$

In the main text, we take  $\epsilon_d = 0$ , to focus on the effect of a left-right asymmetry  $V_L - V_R$ . In this section, we take a finite  $\epsilon_d$ , to study whether the topological-parity degeneracy can also “restore” the detuning, or “particle-hole” asymmetry at the dot.

For the high-temperature situation, Majorana-coupling  $t_M$  is negligible, and RG flow mimics that of a regular DRLM. RG flow equations with a finite  $\epsilon_d$  then become (after reducing the spinful equations of Ref. [S5] to the spinless case)

$$\begin{aligned} \frac{dV_{L,R}}{dl} &= V_{L,R} \left[ 1 - \frac{1+r}{4}(1 + K_{\text{charge}} \pm 2K_{\text{asy}}) \right], \\ \frac{dK_{\text{charge}}}{dl} &= -2\tau_c^2 [K_{\text{charge}}(V_L^2 + V_R^2) + K_{\text{asy}}(V_L^2 - V_R^2)] (e^{\epsilon_d\tau_c} + e^{-\epsilon_d\tau_c}), \\ \frac{dK_{\text{asy}}}{dl} &= -\tau_c^2 [K_{\text{asy}}(V_L^2 + V_R^2) + (V_L^2 - V_R^2)] (e^{\epsilon_d\tau_c} + e^{-\epsilon_d\tau_c}), \\ \frac{d\epsilon_d}{dl} &= \epsilon_d + (V_L^2 + V_R^2)\tau_c (e^{-\epsilon_d\tau_c} - e^{\epsilon_d\tau_c}). \end{aligned} \quad (\text{S10})$$

Clearly a finite  $\epsilon_d$  is RG relevant, and increases when decreasing the temperature. When  $t_M = 0$ , the lead-dot tunnelings are then turned off at zero temperature, where the dot is either fully unoccupied (when  $\epsilon_d < 0$ ), or empty (when  $\epsilon_d > 0$ ). In addition, a finite  $\epsilon_d$ , either positive or negative, accelerates the flow of scaling factors  $K_{\text{asy}}$  and  $K_{\text{charge}}$ . Following Eq. (S10), in the high-temperature regime, a finite dot detuning  $\epsilon_d$  increases the system asymmetry, and tend to sabotage the BKT transition.

In the low-temperature regime, RG flow features above are however greatly modified. Indeed, in this regime, the dot operator has the following influence on the ground states

$$\begin{aligned} d|\psi_1\rangle &= -\frac{i}{2}(\mathcal{A}|\psi_2\rangle + \mathcal{B}|\psi_4\rangle), & d^\dagger|\psi_1\rangle &= \frac{i}{2}(\mathcal{B}|\psi_2\rangle - \mathcal{A}|\psi_4\rangle), \\ d|\psi_2\rangle &= -\frac{i}{2}(\mathcal{A}|\psi_1\rangle + \mathcal{B}|\psi_3\rangle), & d^\dagger|\psi_1\rangle &= \frac{i}{2}(\mathcal{B}|\psi_1\rangle - \mathcal{A}|\psi_3\rangle), \end{aligned} \quad (\text{S11})$$

with two  $\epsilon_d$ -dependent positive parameters

$$\mathcal{A} = \sqrt{1 + \frac{\epsilon_d}{\sqrt{\epsilon_d^2 + 4t_M}}}, \quad \mathcal{B} = \sqrt{\frac{4t_M^2}{4t_M^2 + \epsilon_d(\epsilon_d + \sqrt{\epsilon_d^2 + 4t_M^2})}}. \quad (\text{S12})$$

As the consequence, we obtain the low-temperature RG equations

$$\begin{aligned} \frac{dV_{L,R}}{dl} &= V_{L,R} \left[ 1 - \frac{1+r}{4}(1 + K_{\text{charge}} \pm 2K_{\text{asy}}) \right], \quad \frac{dK_{\text{parity}}}{dl} = -4\mathcal{A}\mathcal{B}\tau_c^2(V_L^2 + V_R^2)K_{\text{parity}}, \\ \frac{dK_{\text{asy}}}{dl} &= -2\mathcal{A}\mathcal{B}\tau_c^2(V_L^2 + V_R^2)K_{\text{asy}}, \quad \frac{dK'_{\text{asy}}}{dl} = -2\mathcal{A}\mathcal{B}\tau_c^2(V_L^2 + V_R^2)K'_{\text{asy}}, \quad \frac{dK_{\text{charge}}}{dl} = 0, \end{aligned} \quad (\text{S13})$$

where the  $\epsilon_d$ -dependent factors  $\mathcal{A}$  and  $\mathcal{B}$  influence the flow of all scaling parameters. However, since  $\mathcal{A}\mathcal{B} > 0$ , the flow patterns of all scaling parameters qualitatively agree with that of the fine-tuned situation, i.e., Eq. (S9), and Eq. (3) of the main text. A finite  $\epsilon_d$  simply modifies the prefactors of RG flow equations. These modifications change only the critical value of  $V_L, V_R$  at the boundary of the transition. The qualitative feature of the phase diagram however remains invariant.

## V. COUPLING THE DRLM DOT TO AN ANDREEV BOUND STATE

In the main text, we have shown that by coupling the dot of a DRLM to an MZM, the BKT QPT hosted by the DRLM will be greatly modified. It is also illustrated and highlighted that the modification of the BKT phase diagram is due to the topological degeneracy provided by the Majorana. To better understand the importance of the topological degeneracy, we consider another example where the dot instead couples to an Andreev bound state (ABS, with the state operator  $d_{\text{ABS}}$ ), with has instead a trivial local degeneracy. Of this case, the impurity part has the Hamiltonian

$$H_{\text{impurity}} = \epsilon_{\text{dot}} d^\dagger d + \epsilon_{\text{ABS}} d_{\text{ABS}}^\dagger d_{\text{ABS}} + t_1 (d_{\text{dot}}^\dagger d_{\text{ABS}} + d_{\text{ABS}}^\dagger d_{\text{dot}}) + t_2 (d_{\text{dot}}^\dagger d_{\text{ABS}}^\dagger + d_{\text{ABS}} d_{\text{dot}}), \quad (\text{S14})$$

where  $t_1 = t_2$  for an MZM. For simplicity we have assumed  $t_1$  and  $t_2$  to be both real numbers. The impurity Hamiltonian has four eigenvalues,

$$\begin{aligned} \epsilon_1 &= \frac{1}{2} \left[ \epsilon_{\text{dot}} + \epsilon_{\text{ABS}} - \sqrt{(\epsilon_{\text{dot}} + \epsilon_{\text{ABS}})^2 + 4t_1^2} \right], & \epsilon_2 &= \frac{1}{2} \left[ \epsilon_{\text{dot}} + \epsilon_{\text{ABS}} - \sqrt{(\epsilon_{\text{dot}} - \epsilon_{\text{ABS}})^2 + 4t_2^2} \right], \\ \epsilon_3 &= \frac{1}{2} \left[ \epsilon_{\text{dot}} + \epsilon_{\text{ABS}} + \sqrt{(\epsilon_{\text{dot}} + \epsilon_{\text{ABS}})^2 + 4t_1^2} \right], & \epsilon_4 &= \frac{1}{2} \left[ \epsilon_{\text{dot}} + \epsilon_{\text{ABS}} + \sqrt{(\epsilon_{\text{dot}} - \epsilon_{\text{ABS}})^2 + 4t_2^2} \right]. \end{aligned} \quad (\text{S15})$$

Apparently, energies  $\epsilon_1$  and  $\epsilon_2$  are candidates of the ground-state energy. If either  $\epsilon_{\text{dot}}$  or  $\epsilon_{\text{ABS}}$  (corresponding to an accidentally fine-tuned ABS) is zero,  $\epsilon_1 \neq \epsilon_2$  and the dot-ABS state reduces an effectively detuned dot: of this case, the BKT QPT does not exist, in great contrast to the enhanced BKT phase diagram of the MZM situation.

Specially, these two energies only equal when  $\epsilon_{\text{dot}}\epsilon_{\text{ABS}} + t_1^2 = t_2^2$ , leading to an accidental degenerate state. We emphasize, however, that this accidental degenerate situation will not sabotage the MZM evidence in real experiments. Indeed, in real experiments, the tuning of  $V_L$  and  $V_R$ , with which the phase diagram is detected, will effectively tune the dot energy  $\epsilon_{\text{dot}}$  [S6] (, and may also influence  $\epsilon_{\text{ABS}}$ ). As the consequence, we expect that the accidental degenerate situation only leads to scattered full-transmission points in phase space, being distinct from the real MZM situation.

Following analysis above, we clearly see that the Majorana-induced modification of the low-temperature RG flow, physically explained in Fig. 3, does require the presence of a topological degeneracy. A fine-tuned trivial ABS ( $\epsilon_{\text{ABS}} = 0$ ) instead leads to always the isolated impurity phase.

---

\* zhanggu@baqis.ac.cn

† dongeliu@mail.tsinghua.edu.cn

- [S1] Dong E. Liu, Huaixiu Zheng, Gleb Finkelstein, and Harold U. Baranger, “Tunable quantum phase transitions in a resonant level coupled to two dissipative baths,” *Phys. Rev. B* **89**, 085116 (2014).
- [S2] Chung-Hou Chung, Karyn Le Hur, Matthias Vojta, and Peter Wölfle, “Nonequilibrium transport at a dissipative quantum phase transition,” *Phys. Rev. Lett.* **102**, 216803 (2009).
- [S3] A. C. Hewson, *The Kondo Problem to Heavy Fermions* (Cambridge Univ. Press, Cambridge UK, 1993).
- [S4] C. L. Kane and Matthew P. A. Fisher, “Transmission through barriers and resonant tunneling in an interacting one-dimensional electron gas,” *Phys. Rev. B* **46**, 15233–15262 (1992).
- [S5] A. Schiller and K. Ingersent, “Renormalization-group study of a magnetic impurity in a luttinger liquid,” *Europhysics Letters* **39**, 645 (1997).
- [S6] H. T. Mebrahtu, I. V. Borzenets, Dong E. Liu, Huaixiu Zheng, Yu. V. Bomze, A. I. Smirnov, H. U. Baranger, and G. Finkelstein, “Quantum phase transition in a resonant level coupled to interacting leads,” *Nature* **488**, 61–64 (2012).